Effective Cancer Therapy with the α-Particle Emitter [^{211}At]Astatine in a Mouse Model of Genetically Modified Sodium/Iodide Symporter–Expressing Tumors

Thorsten Petrich,[1] Leticia Quintanilla-Martinez,[2] Zekiye Korkmaz,[1] Elenore Samson,[2] Hans Jürgen Helmeke,[1] Geerd Jürgen Meyer,[1] Wolfram H. Knapp,[1] and Eyck Pötter[1]

Abstract

Purpose: The *sodium/iodide symporter* (*NIS*) gene is currently explored in several trials to eradicate experimental cancer with radiodine (^{131}I) by its β-emission. We recently characterized NIS-specific cellular uptake of an alternative halide, radioastatine (^{211}At), which emits high-energy α-particles. The aim of this study was to investigate *in vivo* effects of the high linear energy transfer (LET) emitter ^{211}At on tumor growth and outcome in nude mice.

Experimental Design: We administered radioastatide in a fractionated therapy scheme to NMRI nude mice harboring rapidly growing solid tumors established from a papillary thyroid carcinoma cell line genetically modified to express NIS (K1-NIS). Animals were observed over 1 year. Tumor growth, body weight, blood counts, survival, and side effects were measured compared with control groups without therapy and/or lack of NIS expression.

Results: Within 3 months, radioastatide caused complete primary tumor eradication in all cases of K1-NIS tumor-bearing nude mice (n = 25) with no tumor recurrence during 1 year follow-up. Survival rates of the K1-NIS/^{211}At group were 96% after 6 months and 60% after 1 year, in contrast to those of control groups (maximum survival 40 days).

Conclusion: Our study indicates that ^{211}At represents a promising substrate for NIS-mediated therapy of various cancers either with endogenous or gene transfer-mediated NIS expression.

Sodium/iodide symporter (NIS)–mediated iodide uptake into thyroid follicular cells is an essential step in thyroid hormone biosynthesis forming the basis for diagnosis and therapy of differentiated thyroid cancer with β-particle-emitting radioiodine, Na^{131}I (1, 2). Consistent with clinical findings, NIS is also functionally expressed in gastric mucosa, salivary gland, and lactating mammary gland, in addition to several other tissues that contain NIS mRNA and protein (3, 4). These nonthyroid tissues may be affected by NIS-mediated radionuclide transport but have much lower retention compared with healthy or differentiated cancerous thyroid tissue. Recently, functional NIS expression in breast carcinoma was described in a subgroup of patients; therefore, NIS-mediated radioiodide therapy has been suggested as a future treatment option for such patients (3, 5).

For nonthyroid cancers, the combination of *NIS* gene transfer and radioiodide administration offers an intriguing potential therapeutic approach. Experimental studies in various cancer models indicate that, in general, *NIS* gene transfer leads to radioiodide uptake capacity, but in the absence of cellular mechanisms leading to covalent iodide fixation radioactivity is rapidly lost, e.g., by diffusion through anion channels, limiting intratumoral radiation doses (4, 6–9). Although a variety of studies using ^{131}I or other β-particle emitters (in part using *NIS* gene coupled to various tumor specific promotors) result in high cellular radioiodide uptake, only a few studies report tumoricidal effects in animal cancer models (4, 9–18).

α-Particle-emitting radionuclides are attractive radiopharmaceuticals for targeted cancer therapy, as α-particles are extremely cytotoxic due to their high LET (~100 keV/μm) and potentially highly specific due to their short particle path of a few cell diameters (40-80 μm). But taking into account chemical and biochemical properties, physical half-life, decay schemes, and availability, one may consider only a few α-particle emitters, including ^{211}At, ^{212}Bi, ^{213}Bi, and ^{225}Ac, as realistic candidates for therapeutic applications (19–21). Previously, we characterized the transport kinetics of the halide, [^{211}At]astatide, by NIS, which are similar to those of its chemical relative, iodide (22). [^{211}At]Astatide has a short half-life of 7.2 hours compatible with the relatively short residence times observed in cells transfected with *NIS* gene and unable to synthesize iodine-organic compounds. Furthermore, based on former dose calculations, we suggested that NIS-mediated tumor therapy using the α-emitter ^{211}At might be feasible in a xenograft mouse

Authors' Affiliations: [1]Klinik für Nuklearmedizin, Medizinische Hochschule Hannover, Hanover, Germany; [2]Institut für Pathologie, GSF-Forschungszentrum für Umwelt und Gesundheit, Neuherberg, Germany

Received 7/22/05; revised 11/18/05; accepted 11/30/05.

Grant support: HiLF program of the Medizinische Hochschule Hannover, Germany.

The costs of publication of this article were defrayed in part by the payment of page charges. This article must therefore be hereby marked *advertisement* in accordance with 18 U.S.C. Section 1734 solely to indicate this fact.

Requests for reprints: Eyck Pötter, Department of Nuclear Medicine, Medizinische Hochschule Hanover, Carl-Neuberg-Str.1, 30625 Hannover, Germany. E-mail: eyck.potter@web.de.

©2006 American Association for Cancer Research.

doi:10.1158/1078-0432.CCR-05-1576

Downloaded from http://aacrjournals.org/clincancerres/article-pdf/12/4/1342/1967026/1342.pdf by guest on 08 October 2024

model. Here, we report our results of a first long-term follow-up animal study using [^{211}At]astatide therapy with respect to tumor ablation, survival, and side effects.

Materials and Methods

Production of astatine. ^{211}At was produced in our cyclotron (MC35, Scanditronix, Uppsala, Sweden) according to the ^{209}Bi(α,2n) ^{211}At reaction by irradiation of a natural bismuth metal targets with up to 8 μA of 24.5 MeV α-particles on target for 30 to 90 minutes. ^{211}At was separated from the target by dry distillation at 650°C to 750°C for 30 to 60 minutes in a customized apparatus, collected in 0.02 mol/L Na_2SO_3 to stabilize the $^{211}At^-$ anion and used for experimentation after appropriate dilution as described before (22, 23).

Animals. All animal experiments were done according to German federal laws and the Institutional Animal Care and Use Committee guidelines of the Medizinische Hochschule Hannover. Animals were maintained under pathogen-free conditions with free access to water and standard rodent chow without using thyroid hormone blocking protocols. As previously described (22), we used xenografts of a human papillary thyroid carcinoma cell line, K1 (European Collection of Animal Cell Cultures, Salisbury, United Kingdom), lacking endogenous NIS genetically modified to express NIS under control of the cytomegalovirus promoter (K1-NIS) and of control cells. Tumors were raised in NMRI-nu/nu nude mice aged 3 to 4 weeks by s.c. injection into the right or left flanks of 3×10^6 cells in 0.1 mL PBS. Over a growth phase of 2 to 4 weeks, tumors were allowed to reach volumes of 0.2 to 1.0 mL (measured by caliper rule). Mice (n = 25) then received i.p. injections of 1.0, 0.5, and 1.0 MBq ^{211}At on days 0, 5, and 16, respectively. We used three control groups: (*a*) NMRI nude mice given the same ^{211}At therapy regimen but with tumors raised from mock-transfected K1 cells lacking NIS expression (K1-pCI; n = 5), and NMRI nude mice with (*b*) K1-NIS tumors (n = 6), or (*c*) K1-pCI tumors (n = 4) were not given ^{211}At.

In vitro *uptake of astatide.* As previously described, cellular ^{211}At uptake (1 hour steady-state) was measured in K1-NIS cells and in NIS-negative K1-pCI cells as controls compared with uptake by the well-known NIS-specific inhibitor, $NaClO_4$ (22). Assays were done in triplicate; results are expressed as mean ± SD (n = 4). We showed before that K1 wild-type cells lack both endogenous NIS expression and accumulation of iodide and astatide. We also showed that K1-NIS cells had same fast washout kinetics of accumulated radionuclides as other NIS-transfected nonthyroid carcinoma cells (22). Other authors showed that K1 cells did not express other thyroid-specific genes (e.g., thyroid peroxidase, TSH receptor; ref. 24 and references therein). Thus, K1 may be regarded for the purpose of this study as a suitable model for dedifferentiated thyroid cancer.

Therapy follow-up. In all animal groups, we measured tumor size and body weight and photographed each individual every week. Animals were sacrificed when tumors exceeded sizes of 20 mm or volumes of 4 mL or when major symptoms (e.g., cachexia, apathy, paralysis, and ileus) appeared. In all surviving K1-NIS/^{211}At mice, we did planar $^{99m}TcO_4^-$ scintigraphy for tumor and thyroid uptake 1 hour after i.p. injection of 10 MBq $^{99m}TcO_4^-$/0.1 mL 0.9%NaCl at 7 months by using a γ-camera system (ZLC370, Siemens, Malvern, PA) with a LEAP collimator. [^{99m}Tc]Pertechnetate, a NIS substrate but not organified in thyroid hormone biosynthesis, is often used for thyroid, gastric, and salivary gland scans due to its favorable imaging qualities, short effective half-life, and low radiation dose. Blood counts were analyzed at 4 (n = 25), 6 (n = 8), and 12 months (n = 10) after onset of therapy for values of white and RBC, platelets, hemoglobin concentration, hematocrit, and mean corpuscular volume compared with normal untreated nude mice (results shown as mean ± 2 SD).

Histology. K1-NIS/^{211}At mice were analyzed for therapy side effects or residual tumor tissue by histology compared with normal animals. Therefore, mice were killed at the end of the observation period (maximum of 1 year) and prepared for transport to GSF-Forschungszentrum (Neuherberg, Germany) by formalin fixation. In GSF, organs were removed and embedded in paraffin. Microscopic analysis for pathologic changes was done with H&E-stained sections of all organs.

Biodistribution. To determine the *in vivo* distribution of ^{211}At, K1-NIS solid tumor-bearing nude mice (n = 6, tumor sizes, 0.2-0.7 mL) were killed 2 hours after i.p. injection of 1.3 to 1.8 MBq ^{211}At. Organs were removed, weighed, and their radioactivity was determined. Results are expressed as percentage of injected dose per gram of tissue.

Statistics. Survival analysis was done according to Kaplan-Meier using SPSS Software and log-rank test for comparisons between therapy groups. Paired and grouped t tests were used for cellular astatine uptake, biodistribution, and body weight. Variant analysis using Scheffe's procedure was used for blood values. $P < 0.05$ were considered to indicate significant differences.

Results

In vitro *cellular ^{211}At uptake and biodistribution.* *In vitro*, cellular ^{211}At uptake was high only in K1-NIS cells and could specifically be blocked by 150 μmol/L $NaClO_4$, a known competitive inhibitor of NIS-mediated transport (Fig. 1A). In the mouse model, biodistribution experiments showed the highest uptake of ^{211}At in K1-NIS tumor tissue, followed by the neck (including the thyroid), lung, stomach, and spleen (Fig. 1B).

Therapy, follow-up, and survival. In a preliminary dose-finding study (data not shown), we used ^{211}At and ^{131}I in NMRI nude mice bearing K1-NIS tumors (25). Compared with controls without therapy (n = 3), an initial retardation of tumor growth for 5 weeks followed by rapid growth of the tumor were observed after ^{131}I administration (25 MBq, n = 3). However,

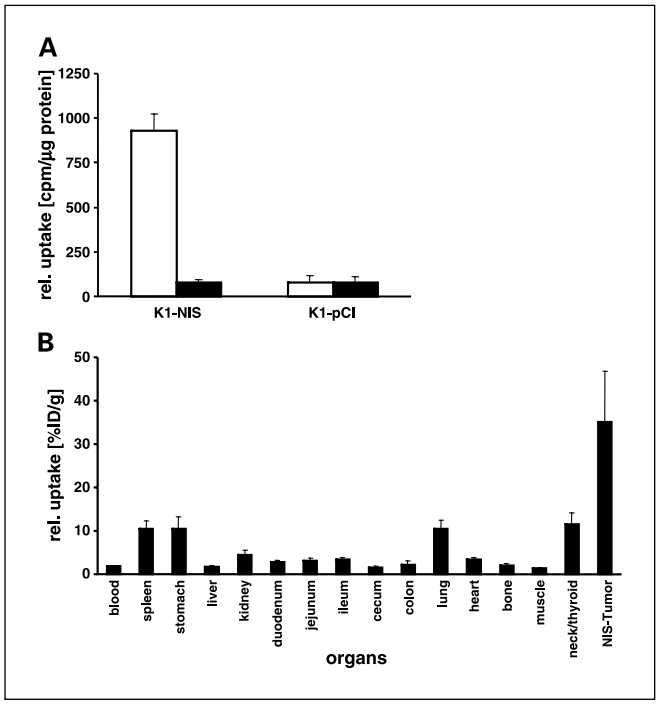

Fig. 1. *In vitro* and *in vivo* specific ^{211}At uptake. *A, in vitro*, cellular ^{211}At uptake (1 hour steady-state, *white columns*) is high in K1-NIS cells but not in NIS-negative K1-pCI cells ($P < 0.0001$, grouped t test) and is suppressed by the NIS inhibitor $NaClO_4$ (*black columns*, $P < 0.0001$, grouped t test; mean ± SD, n = 4, assays done in triplicate). *B,* biodistribution of ^{211}At in K1-NIS solid tumor-bearing nude mice after organ removal 2 hours after i.p. injection of ^{211}At expressed as percentage of injected dose per gram of tissue. K1-NIS tumors significantly take up more ^{211}At compared with other tissues ($P < 0.005$, paired t test and $P < 0.01$ Bonferroni t test).

Downloaded from http://aacrjournals.org/clincancerres/article-pdf/12/4/1342/1967026/1342.pdf by guest on 08 October 2024

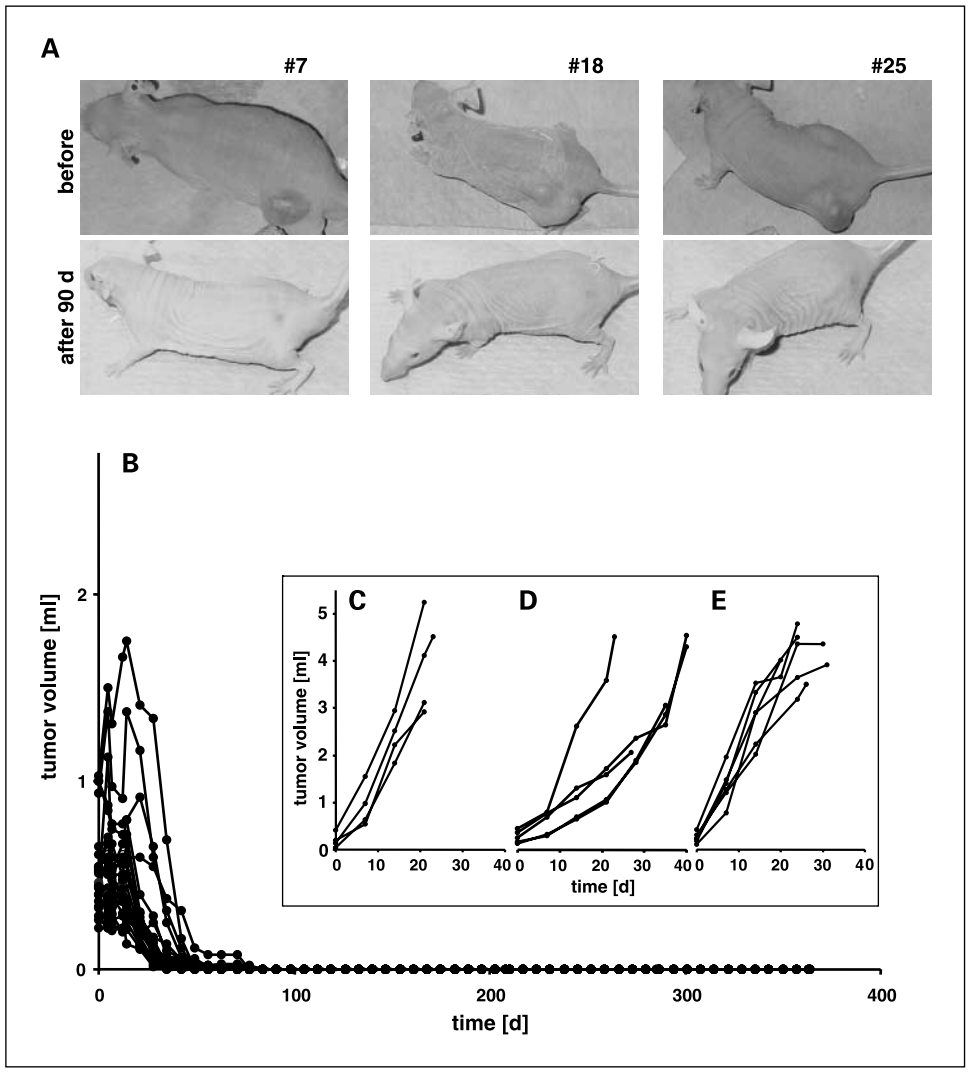

Fig. 2. Tumor response after ^{211}At therapy of K1-NIS mice and controls. *A,* photographs of three representative K1-NIS tumor-bearing nude mice (*top*) demonstrating complete tumor regression (*bottom*) 90 days after fractionated ^{211}At therapy (1, 0.5, and 1 MBq injected i.p. on days 0, 5, and 16, respectively). Scar and skin hyperpigmentation are visible at the tumor implantation site. *B,* ^{211}At therapy leads to complete clinical tumor remission in K1-NIS mice (n = 25, initial tumor volumes, 0.2-1.0 mL) within 90 days, with no local tumor recurrence through 1 year follow-up, in contrast to rapid growth in control groups [*insets: C,* K1-pCI tumor (n = 4); *D,* K1-pCI tumor with ^{211}At therapy (n = 5); *E,* K1-NIS tumor without ^{211}At therapy (n = 6)].

radioastatine (1 MBq, n = 3) caused tumor shrinkage followed by stable disease up to 8 weeks but then tumor regrowth started (25). A higher activity of ^{131}I was used as dose calculations indicated 15- to 20-fold higher radiation dose per administered radioactivity of ^{211}At compared with ^{131}I (22).

The preliminary study mentioned above indicated insufficient dose for tumor elimination; thus, we developed a fractionated ^{211}At therapy scheme (see Materials and Methods) allowing for higher dose delivery. After ^{211}At administration (2.5 MBq total applied activity) according to that scheme, K1-NIS tumors showed complete remission (examples in Fig. 2A) within 90 days, without recurrence in the observation period, whereas controls had rapid tumor growth with a maximum survival of 40 days (Fig. 2B-E). The survival rate of K1-NIS/^{211}At mice (96%/60% at 6/12 months) was significantly higher than that of control groups (P < 0.0001, log-rank test; Fig. 3A). After ^{211}At therapy, all K1-NIS mice had normal social and feeding behavior without diarrhea or obstipation or major hypothyroid symptoms. Body weights of K1-NIS mice increased after ^{211}At treatment; in contrast, body weights of controls decreased due to cachexia necessitating sacrifice (Fig. 4). All measured blood counts in K1-NIS/^{211}At mice were within reference ranges for NMRI nude mice (Fig. 5). No significant signs for bone marrow depression except slight changes in hemoglobin concentration were determined in the peripheral blood. Also, no general clinical signs (i.e., petechial bleeding or lethargy) were evident.

Monitoring* in vivo *tumor growth by scintigraphy. Scintigraphy showed high $^{99m}TcO_4^-$ uptake in K1-NIS tumors in untreated controls (Fig. 3B), but no tumor-specific uptake in K1-NIS/^{211}At mice 7 months after therapy due to complete tumor remission (Fig. 3C). However, thyroid function determined by radionuclide uptake was decreased to different levels in the K1-NIS/^{211}At mice indicating thyroid damage.

Histology and side effects after ^{211}At therapy. Histologic findings (n = 23; Fig. 6) showed no tumor residues at the primary tumor site in 21 of 23 K1-NIS/^{211}At mice. Two K1-NIS/^{211}At mice had microscopic tumor residues at that site without proliferation, and an additional mouse had a microscopic local i.m. residual tumor node without proliferation or tumor invasion. Other histopathologic findings included effects on the thyroid (atrophy in all mice), liver [foci of atypical hepatocytes (n = 11), adenoma (n = 2), and differentiated carcinoma (n = 4)], spleen (increased erythropoiesis, n = 7), lung (inflammation, n = 6), stomach/bowel

Downloaded from http://aacrjournals.org/clincancerres/article-pdf/12/4/1342/1967026/1342.pdf by guest on 08 October 2024

[inflammation (n = 5), hyperplasia (n = 5), atypical cells (n = 4), and papillomas (n = 2)], and skin (angiosarcoma, n = 4). One mouse had acute myeloid leukemia; another had an ovarian granulosa cell tumor.

Discussion

Here, we exploited the limited ion selectivity of NIS and a special feature of the α-emitter ^{211}At, its biochemical similarity to iodine, for direct delivery of radiotherapy into NIS-expressing tumors. In cellular models, we and others have shown before that [^{211}At]astatide is actively transported across the plasma membrane into the cytoplasm by NIS (22, 26, 27). Consistent with these data, we showed in the present study high tumor uptake of ^{211}At in the presence of NIS expression in a mouse model of thyroid carcinoma, whereas control cells transfected with empty vectors were unable to specifically accumulate the radionuclide. A total activity of 2.5 MBq ^{211}At (100 kBq/g body weight; mean body weight 25 g) given in three fractions eliminated advanced NIS tumors in all animals and resulted in a significantly improved survival relative to untreated controls. In the K1-NIS/^{211}At group, no animal died from tumor progression. We are not aware of experimental studies using NIS in combination with radionuclide therapy reporting a comparable complete tumor elimination coupled to high survival with follow-up over 1 year. The mortality rates in our mice given high-dose ^{211}At treatment are in accordance with reported LD_{10} values (dose killing 10% of healthy animals per year) in ^{211}At dose escalation studies in B6C3F1 and BALB/c (nu/nu) mice (28).

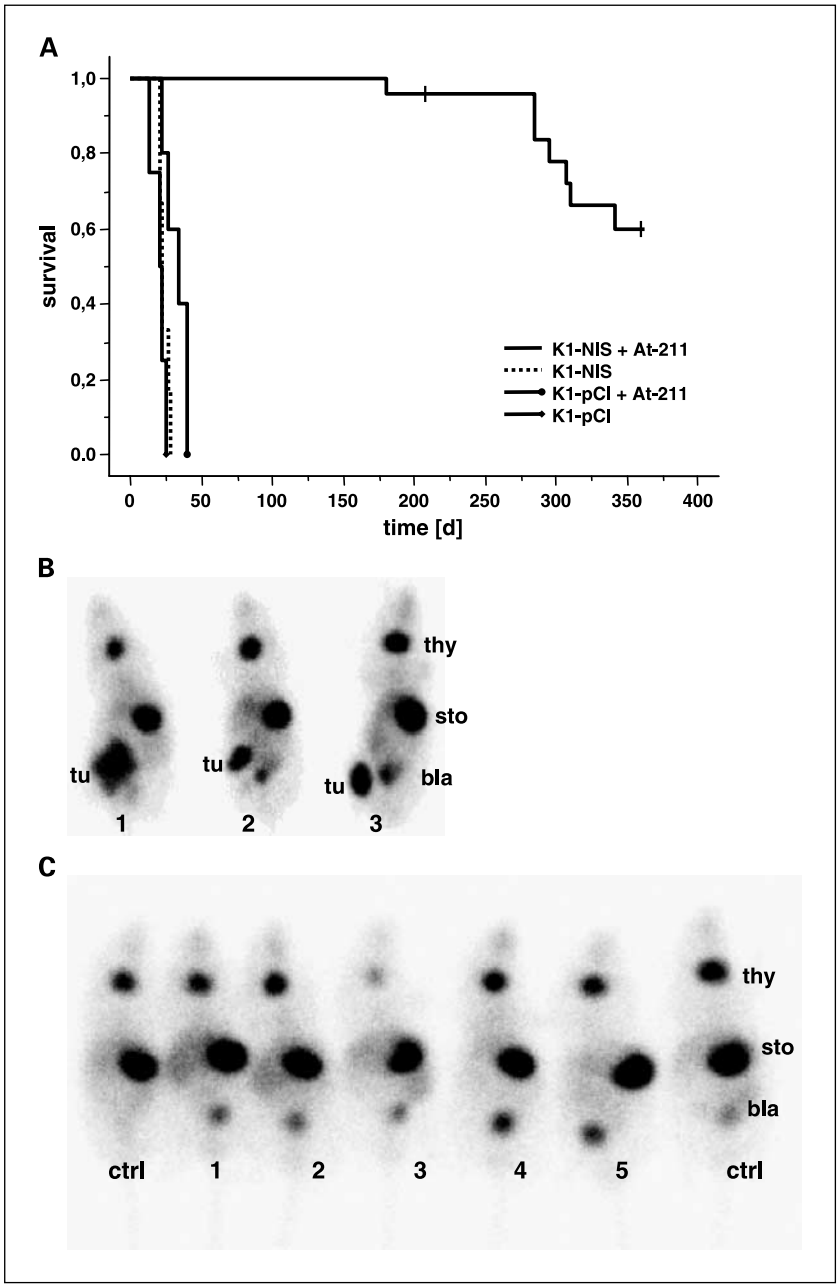

Fig. 3. Survival and therapy monitoring after ^{211}At therapy. *A*, survival of K1-NIS tumor-bearing nude mice (n = 25) after ^{211}At therapy and of control groups, K1-pCl tumor (n = 4), K1-pCl tumor with ^{211}At therapy (n = 5), and K1-NIS tumor without ^{211}At therapy (n = 6). K1-NIS mice receiving ^{211}At therapy had significant prolonged survival compared with controls ($P < 0.0001$, log-rank test). Planar scintigraphy of K1-NIS tumor-bearing nude mice before (mice 1-3, *B*) and 7 months after ^{211}At therapy [mice 1-5, plus two additional untreated control parental mice (*ctrl*), *C*] obtained after 10 MBq $^{99m}TcO_4^-$ 1 hour i.p. Tumor (*tu*) is located in right flank (*B*). Seven months posttreatment, scintigraphy shows no evidence of local disease; however, mouse 3 shows strongly decreased thyroid uptake (*C*). Physiologic uptake is apparent in thyroid (*thy*), stomach (*sto*), and bladder (*bla*) viewed from the ventral side.

Downloaded from http://aacrjournals.org/clincancerres/article-pdf/12/4/1342/1967026/1342.pdf by guest on 08 October 2024

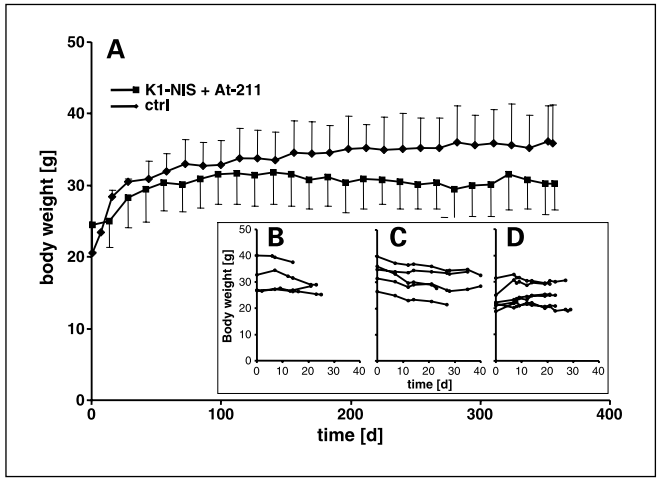

Fig. 4. Body weight effects of ^{211}At therapy. *A,* body weights of K1-NIS tumor-bearing mice (n = 25) increase during ^{211}At therapy and after complete remission but do not reach those of parental nude mice (*ctrl*, n = 6). Body weight differences of NMRI nude mice and ^{211}At-treated K1-NIS mice were not significant before day 250 (time interval days: 0-30, 31-140, and 141-250, $P > 0.05$) and significant at the end of measurement (time interval days 251-365, $P = 0.014$, grouped t test). Control groups display body weight loss during tumor growth: *B*, K1-pCI tumor (n = 4); *C*, K1-pCI tumor after ^{211}At therapy (n = 5); *D*, K1-NIS tumor without ^{211}At therapy (n = 6).

Regarding side effects of ^{211}At therapy, histopathology revealed normal tissue damage and secondary tumors in some animals in our study 6 to 12 months after therapy onset. Thyroid atrophy as found in all animals can be explained by physiologic NIS expression and NIS-dependent ^{211}At uptake of thyrocytes. The secondary tumor spectrum we observed may have several causes. One possibility is that ^{211}At induced carcinogenesis; as in other studies, various tumors have been found after injection of comparable amounts per gram body weight of ^{211}At in mice but tumor incidence was not significantly elevated compared with aging control mice (28, 29). To our knowledge, there are only scant specific data available about tumor diseases in the derived athymic NMRI-nu/nu nude mice strain that we used. In one study, no tumor growth within 7 months was reported, but all animals in the study died after a maximum survival of 7 months due to inflammation of the colon (30). There is no further study available describing tumor incidence after a time period of >7 months. However, the background NMRI mouse strain spontaneously develops diverse tumors of lung, liver, ovary, and hematopoetic system with increasing age (31). Under the assumption that NMRI nude mice like the NMRI strain are prone to a certain tumor spectrum on aging (i. e. without any therapeutic intervention), it is likely that some late tumors we observed in surviving animals are not due to ^{211}At therapy. But solving this question would require to examine a great number ($\gg$100) of animals for pathologic changes what is beyond the scope of this study. Here, we only observed a small control group without At therapy (n = 6) for measurement of body weight over 1 year. No tumors were macroscopically evident but these mice were not examined by histology.

Whether direct ^{211}At toxicity to normal tissue by specific (e.g., thyroid) or unspecific absorption (e.g., liver, skin, and ovary) or possible indirect toxicity caused by ^{211}At-mediated thyroid dysfunction is responsible for side effects has to be clarified in further dose escalation studies using ^{211}At in combination with T4-mediated TSH suppression to decrease TSH-dependent NIS expression in the thyroid and hypothyroidism. Furthermore, the efficacy of low-dose ^{211}At regimens needs to be examined to optimize the relation of survival and side effects. With respect to conceivable ^{211}At therapy in humans, such low-dose regimens may improve efficacy of radionuclide therapy of thyroid carcinomas or its metastases in which ^{131}I uptake is detectable but insufficient for tumor eradication.

Although side effects are documented here, the therapeutic effect increases survival significantly. In other animal studies

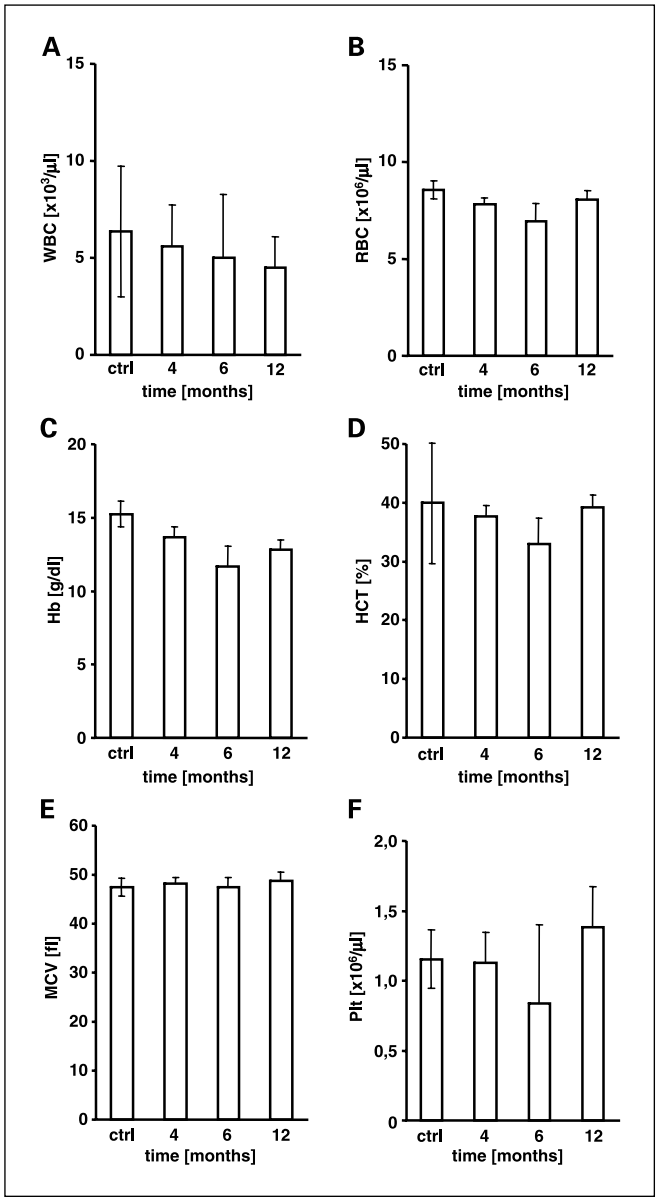

Fig. 5. Hematologic effects of ^{211}At therapy. Hematologic values in ^{211}At-treated K1-NIS tumor-bearing mice after 4, 6, and 12 months compared with untreated parental mice (*ctrl*). Columns, reference range, mean; bars, 2 SD. Values of WBC (*A*), RBC (*B*), platelets (*C*), hemoglobin concentration (*D*), hematocrit (*E*), and mean corpuscular volume (*F*) were within reference ranges (no significant differences in values after 12 months versus controls, variant analysis, and Scheffe's procedure except hemoglobin concentration due to very low SDs).

Downloaded from http://aacrjournals.org/clincancerres/article-pdf/12/4/1342/1967026/1342.pdf by guest on 08 October 2024

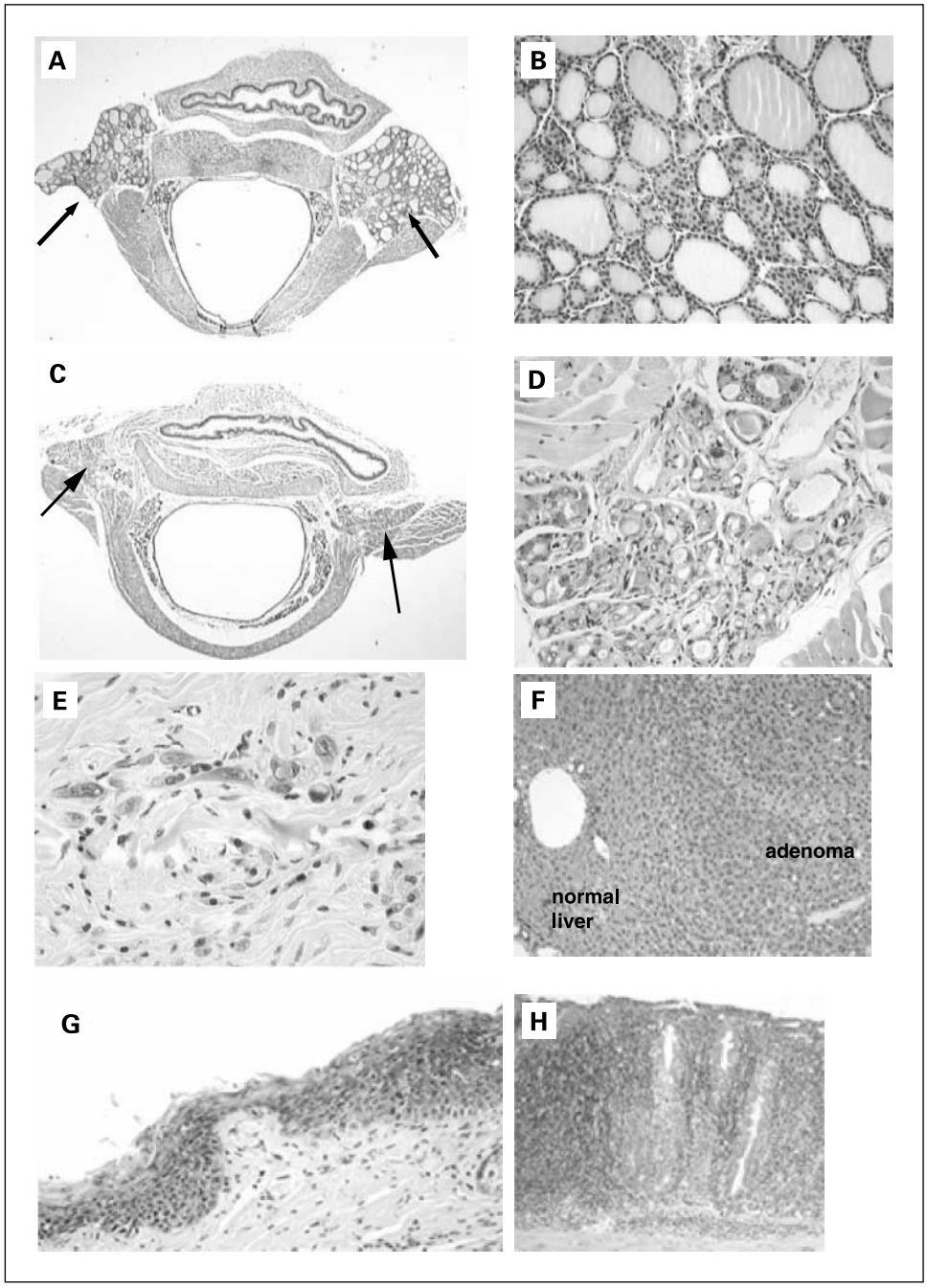

Fig. 6. Histologic findings in ^{211}At-treated K1-NIS mice. Normal thyroid of controls (*A* and *B*) and organ histopathology 208 days (*C-E*) and 363 days (*F-G*) after ^{211}At treatment. The thyroid glands, which were not protected by TSH-suppressive hormone therapy to down-regulate NIS expression, show atrophy in all (23 of 23) examined animals (*C* and *D*). All mice had scar tissue in the flanks with increased number of hemosiderin-laden macrophages explaining skin hyperpigmentation at the tumor implantation site. In 2 of 23 animals, microscopic deposits of residual tumor cells were detected (*E*) in scar tissue of the flank, without macroscopic tumor nodules. One animal had a stable 4 mm residual tumor in the flank (sacrificed 208 days after treatment, not shown). Alterations of the liver included adenoma (*F*; measured 208 days after treatment), hepatocarcinomas (measured 296-363 days after treatment), and granulomas (285 days after treatment). Additional histopathology included severe dysplasia of the epidermis (*G*) 208 to 363 days after treatment and severe inflammation of the colon with atypical regenerative changes (*H*).

with different NIS-expressing systems, using β-emitters such as ^{131}I or ^{188}Re, mostly tumor growth retardation or partial remission followed by tumor regrowth was measured (9, 11, 15, 16, 18, 32).

The high tumor toxicity in our results coupled to lack of acute side effects and to only moderate late side effects is most likely explainable by NIS-dependent effective cellular [^{211}At]astatide accumulation resulting in a high probability of an intracellular α-decay with a short path length of the α-particle. Thereby, DNA-damaging effects of emitted high LET α-particles are enhanced by intracellular recoil effects of the emitting astatide nuclei. In addition, the extreme high LET of α-emitters and recoil effects of the intracellular/intranuclear decay compared with much lower LET of β-emitters causes significant higher damage of various cellular proteins in direct contact to sensitive cytoplasmic metabolic processes, which are irreplaceable for cell survival. It is assumed that as few as four α-particles traversing the nucleus are sufficient to eliminate a cell (33–35).

In our study, we used a tumor model with NIS overexpression that results in a high therapeutic outcome and relatively low side effects after systemic ^{211}At administration. A few promising therapy studies using radiodine using viral vectors with tissue-specific promoters targeting NIS to tumor cells in animals have already been done in combination with ^{131}I therapy (10, 32, 36–38). It may be worth to consider that use of ^{211}At in these existing models may improve the results.

Downloaded from http://aacrjournals.org/clincancerres/article-pdf/12/4/1342/1967026/1342.pdf by guest on 08 October 2024

However, it has to been taken into account that up to now, *in vivo* gene therapy approaches and other cell targeting methods, e.g., labeled antibodies, do not have sufficient specificity to prevent all nontargeted tissues from late side effects.

Another aspect of the attraction of astatine for prospective use in clinical settings is the short half-life (7.2 hours of ^{211}At versus 8 days of ^{131}I) and the short range of α-particles that would make exposure to nonpatient personnel minimal. Provided that low-dose ^{211}At regimens could be established to result in minimal side effects, therapy of goiter and hyperthyroidism (tissue with high endogenous NIS expression) might also be feasible substituting radioiodide by radioastatide. In conclusion, the results of our proof-of-principle study underscore the potential of high LET α-emitter [^{211}At]astatide for cytoreductive NIS-mediated therapy of malignant tumors. ^{211}At proved to have a high tumoricidal potential in *NIS* gene–transfected tumors without major side effects limiting survival in mice. Thus, apart from potential use in tumors with endogenous NIS expression, ^{211}At seems attractive for further evaluation in targeted NIS-mediated cancer gene therapy studies.

Acknowledgments

We thank H. Geerlings (Institute of Biometry, Medizinische Hochschule Hannover, Hannover, Germany) for help with statistical analysis.

References

1. Dai G, Levy O, Carrasco N. Cloning and characterization of the thyroid iodide transporter. Nature 1996; 379:458–60.
2. Mazzaferri EL, Kloos RT. Clinical review 128: current approaches to primary therapy for papillary and follicular thyroid cancer. J Clin Endocrinol Metab 2001;86: 1447–63.
3. Tazebay UH, Wapnir IL, Levy O, et al. The mammary gland iodide transporter is expressed during lactation and in breast cancer. Nat Med 2000;6:871–8.
4. Spitzweg C, Morris JC. The sodium iodide symporter: its pathophysiological and therapeutic implications. Clin Endocrinol (Oxf) 2002;57:559–74.
5. Wapnir IL, Goris M, Yudd A, et al. The Na^+/I^- symporter mediates iodide uptake in breast cancer metastases and can be selectively down-regulated in the thyroid. Clin Cancer Res 2004;10:4294–302.
6. Shimura H, Haraguchi K, Miyazaki A, Endo T, Onaya T. Iodide uptake and experimental ^{131}I therapy in transplanted undifferentiated thyroid cancer cells expressing the Na^+/I^- symporter gene. Endocrinology 1997;138:4493–6.
7. Mandell RB, Mandell LZ, Link CJ, Jr. Radioisotope concentrator gene therapy using the sodium/iodide symporter gene. Cancer Res 1999;59:661–8.
8. Boland A, Ricard M, Opolon P, et al. Adenovirus-mediated transfer of the thyroid sodium/iodide symporter gene into tumors for a targeted radiotherapy. Cancer Res 2000;60:3484–92.
9. Smit JW, Schroder-van der Elst JP, Karperien M, et al. Iodide kinetics and experimental (131)I therapy in a xenotransplanted human sodium-iodide symporter-transfected human follicular thyroid carcinoma cell line. J Clin Endocrinol Metab 2002;87: 1247–53.
10. Spitzweg C, O'Connor MK, Bergert ER, Tindall DJ, Young CY, Morris JC. Treatment of prostate cancer by radioiodine therapy after tissue-specific expression of the sodium iodide symporter. Cancer Res 2000;60: 6526–30.
11. Cho JY, Shen DH, Yang W, et al. *In vivo* imaging and radioiodine therapy following sodium iodide symporter gene transfer in animal model of intracerebral gliomas. Gene Ther 2002;9:1139–45.
12. Kakinuma H, Bergert ER, Spitzweg C, Cheville JC, Lieber MM, Morris JC. Probasin promoter (ARR(2)PB)-driven, prostate-specific expression of the human sodium iodide symporter (h-NIS) for targeted radioiodine therapy of prostate cancer. Cancer Res 2003;63:7840–4.
13. Schipper ML, Weber A, Behe M, et al. Radioiodide treatment after sodium iodide symporter gene transfer is a highly effective therapy in neuroendocrine tumor cells. Cancer Res 2003;63:1333–8.
14. Faivre J, Clerc J, Gerolami R, et al. Long-term radioiodine retention and regression of liver cancer after sodium iodide symporter gene transfer in Wistar rats. Cancer Res 2004;64:8045–51.
15. Mitrofanova E, Unfer R, Vahanian N, et al. Rat sodium iodide symporter for radioiodide therapy of cancer. Clin Cancer Res 2004;10:6969–76.
16. Shen DH, Marsee DK, Schaap J, et al. Effects of dose, intervention time, and radionuclide on sodium iodide symporter (NIS)-targeted radionuclide therapy. Gene Ther 2004;11:161–9.
17. Scholz IV, Cengic N, Baker CH, et al. Radioiodine therapy of colon cancer following tissue-specific sodium iodide symporter gene transfer. Gene Ther 2005; 12:272–80.
18. Dadachova E, Nguyen A, Lin EY, Gnatovskiy L, Lu P, Pollard JW. Treatment with rhenium-188-perrhenate and iodine-131 of NIS-expressing mammary cancer in a mouse model remarkably inhibited tumor growth. Nucl Med Biol 2005;32:695–700.
19. McDevitt MR, Sgouros G, Finn RD, et al. Radioimmunotherapy with α-emitting nuclides. Eur J Nucl Med 1998;25:1341–51.
20. McDevitt MR, Ma D, Lai LT, et al. Tumor therapy with targeted atomic nanogenerators. Science 2001; 294:1537–40.
21. Zalutsky MR. Targeted radiotherapy of brain tumours. Br J Cancer 2004;90:1469–73.
22. Petrich T, Helmeke HJ, Meyer GJ, Knapp WH, Potter E. Establishment of radioactive astatine and iodine uptake in cancer cell lines expressing the human sodium/iodide symporter. Eur J Nucl Med Mol Imaging 2002;29:842–54.
23. Helmeke HJ, Mahnke E, Schaardt U, Knapp WH. External targets for the production of ^{211}At-review and status of the target development at the Hannover cyclotron. Z Med Phys 2004;14:195–9.
24. Wyllie FS, Haughton MF, Rowson JM, Wynford-Thomas D. Human thyroid cancer cells as a source of isogenic, isophenotypic cell lines with or without functional p53. Br J Cancer 1999;79:1111–20.
25. Petrich T, Helmeke HJ, Meyer GJ, Knapp WH, Potter E. Biodistribution and therapeutic outcome after At-211 and I-131 treatment in a mouse model of xenografted sodium/iodide-symporter- expressing thyroid tumor cells. Eur J Nucl Med 2002; 29:S166; V441.
26. Carlin S, Akabani G, Zalutsky MR. *In vitro* cytotoxicity of (211)At-astatide and (131)I-iodide to glioma tumor cells expressing the sodium/iodide symporter. J Nucl Med 2003;44:1827–38.
27. Lindencrona U, Nilsson M, Forssell-Aronsson E. Similarities and differences between free ^{211}At and ^{125}I-transport in porcine thyroid epithelial cells cultured in bicameral chambers. Nucl Med Biol 2001;28: 41–50.
28. McLendon RE, Archer GE, Garg PK, Bigner DD, Zalutsky MR. Radiotoxicity of systematically administered [^{211}At]astatide in B6C3F1 and BALB/c (nu/nu) mice: a long-term survival study with histologic analysis. Int J Radiat Oncol Biol Phys 1996;35:69–80.
29. McLendon RE, Archer GE, Larsen RH, Akabani G, Bigner DD, Zalutsky MR. Radiotoxicity of systemically administered ^{211}At-labeled human/mouse chimeric monoclonal antibody: a long-term survival study with histologic analysis. Int J Radiat Oncol Biol Phys 1999;45:491–9.
30. Rehm S, Deerberg F, Sickel E. Spontaneous diseases and pathologic changes in Han: NMRI nu/nu mice. Z Versuchstierkd 1980;22:309–16.
31. Rittinghausen S, Kaspareit J, Mohr U. Incidence and spectrum of spontaneous neoplasms in Han:NMRI mice of both sexes. Exp Toxicol Pathol 1997;49:347–9.
32. Mitrofanova E, Unfer R, Vahanian N, Kane S, Carvour M, Link C. Effective growth arrest of human colon cancer in mice, using rat sodium iodide symporter and radioiodine therapy. Hum Gene Ther 2005; 16:1333–7.
33. Macklis RM, Lin JY, Beresford B, Atcher RW, Hines JJ, Humm JL. Cellular kinetics, dosimetry, and radiobiology of α-particle radioimmunotherapy: induction of apoptosis. Radiat Res 1992;130:220–6.
34. Imam SK. Advancements in cancer therapy with α-emitters: a review. Int J Radiat Oncol Biol Phys 2001; 51:271–8.
35. Mulford DA, Scheinberg DA, Jurcic JG. The promise of targeted {α}-particle therapy. J Nucl Med 2005;46 Suppl 1:199–204S.
36. Dwyer RM, Bergert ER, O'Connor MK, Gendler SJ, Morris JC. *In vivo* radioiodide imaging and treatment of breast cancer xenografts after MUC1-driven expression of the sodium iodide symporter. Clin Cancer Res 2005;11:1483–9.
37. Dingli D, Diaz RM, Bergert ER, O'Connor MK, Morris JC, Russell SJ. Genetically targeted radiotherapy for multiple myeloma. Blood 2003;102:489–96.
38. Dingli D, Peng KW, Harvey ME, et al. Image-guided radiovirotherapy for multiple myeloma using a recombinant measles virus expressing the thyroidal sodium iodide symporter. Blood 2004;103:1641–6.

Downloaded from http://aacrjournals.org/clincancerres/article-pdf/12/4/1342/1967026/1342.pdf by guest on 08 October 2024